Збірник праць Інституту математики НАН України 2013, т. 10, № 3, 262–283

УДК 532.595

Sloshing in a two-dimensional circular tank. Weakly-nonlinear modal equations *

M.O. Chernova [1], ***A.N. Timokha*** [2]

[1] *Bogomolets National Medical University, Kiev;*
family_ 05@voliacable.com
[2] *Institute of Mathematics of NAS of Ukraine; Kiev, tim@imath.kiev.ua*

Weakly-nonlinear modal equations are derived for modeling the liquid sloshing dynamics in a two-dimensional circular tank by using analytically-approximate natural sloshing modes and Lukovsky' nonconformal mapping technique.

Используя специальные приближения собственных форм и технику неконформных отображений Луковского, выводятся слабонелинейные модальные уравнения, моделирующие динамику жидкости в круговом баке.

Виводяться слабонелінійні модальні рівняння для моделювання динаміки рідини в круговому баці, використовуючи спеціальні наближення власних форм та техніку неконформних відображень Луковского.

1 Introduction

Understanding the liquid sloshing behavior requires combining analytical and computational fluid dynamics (CFD) as well as model tests. Being motivated in analyzing the liquid sloshing response in lorry tanks, horizontal cylindrical ship tanks, railway cisterns, and storage containers exposed to seismic excitations, several researchers conducted experimental and theoretical studies [1,3,4,13,16,18,21] on sloshing in two-dimensional circular tanks focusing on both transient and steady-state regimes. An almost full review of the theoretical results can be found in recent papers [10, 14] which reflect the disregarding fact that the theoretical studies

* This work was supported by Research work № 0112U001015

are mainly restricted to the linear statement or, alternatively, perform *ad hoc* simulations by using different open-source and commercial packages. The present paper is, probably, the first attempt towards creating a semi-analytical theory of nonlinear sloshing in a two-dimensional tank by using the nonlinear multimodal method. Normally, the method provides rather accurate results for hydrodynamic characteristics and loads within theoretical assumptions on irrotational flow of an incompressible fluid with single-valued free surface elevations. The weakly-nonlinear modal systems derived by the method have all attributes of an analytical theory so that studying the modal equations makes it possible to get an insight into the physics of liquid flows, e.g., by analyzing the energy distribution and transfer between the natural sloshing modes, jumps between steady-state solution branches and hydrodynamic instability.

The nonlinear multimodal method has been extensively elaborated for tanks with vertical walls when there exist exact analytical natural sloshing modes and the single-valued free surface elevations are handled by the normal free-surface representation $z = f(x, y, t)$. Examples are upright circular, and two-dimensional and three-dimensional rectangular tanks [9]. The two-dimensional circular tank is not the case. When deriving a *linear* modal theory, the paper [10] pointed out two principal difficulties for generalizing the results to the nonlinear case. The first difficulty is a requirement in approximate analytical natural sloshing modes which are harmonic functions (satisfying the Laplace equation) not only in the mean liquid domain but also in the whole tank interior and, in addition, exactly satisfy the body-boundary conditions for all admissible positions of the free surface. The papers [10, 11] constructed the appropriate approximate natural sloshing modes. The second difficulty is that the circular shape does not admit the normal [single-valued] parametrization of the free surface which is required for the nonlinear multimodal method. In the present paper, we will show that one can use the so-called nonconformal mapping technique by Lukovsky [15] (combined with the Bateman–Luke variational formulation) for getting a single-valued parametrization and derivation of the so-called adaptive nonlinear modal equations.

When assuming a harmonic resonant excitation of the lowest natural sloshing mode, the adaptive modal equations transform to the Narimanov-Moiseev form. Applicability of the Narimanov-Moiseev modal equations depends on whether a secondary resonance may occur due to amplification of the second and third harmonics in the corresponding higher modes. The secondary resonance occurrence is examined. The forthcoming studies should focus on the steady-state analysis of the nonlinear resonant sloshing.

2 Statement of the problem

2.1 Free boundary problem

We consider forced transversal surface waves in a horizontal circular cylindrical tank of radius R_0. The liquid is ideal incompressible with irrotational flow. For brevity, we focus in the present paper on translatory horizontal excitations with a relatively small magnitude.

The analysis will be done in nondimensional statement which suggests characteristic dimension R_0 and time $t_* = \sqrt{R_0/g}$ where g is the gravity acceleration. This implies that the theoretical tank has the unit radius and the introduced horizontal tank displacements $\eta_2(t)$ are already scaled by R_0. The corresponding nondimensional free-boundary problem is formulated in the *tank-fixed* coordinate system Oyz with the origin in the circle center. The nondimensional *absolute liquid velocity* is described by the velocity potential $\Phi(y, z, t)$ and the unknown function $Z(y, z, t)$ describes the instant free surface shape $\Sigma(t)$ by the equation $Z(y, z, t) = 0$. The free-boundary problem is formulated with respect to the unknowns Φ and Z and takes the form

$$\frac{\partial^2\Phi}{\partial y^2} + \frac{\partial^2\Phi}{\partial z^2} = 0 \quad \text{in} \quad Q(t), \tag{1a}$$

$$\frac{\partial\Phi}{\partial n} = \dot{\eta}_2 n_2 \quad \text{on} \quad S(t), \tag{1b}$$

$$\frac{\partial\Phi}{\partial n} = \dot{\eta}_2 n_2 - \frac{\partial Z}{\partial t}\Big/|\nabla Z| \quad \text{on} \quad \Sigma(t), \tag{1c}$$

$$\frac{\partial\Phi}{\partial t} + \tfrac{1}{2}(\nabla\Phi)^2 - \frac{\partial\Phi}{\partial y}\dot{\eta}_2 + z = 0 \quad \text{on} \quad \Sigma(t), \tag{1d}$$

$$\int_{Q(t)} \mathrm{d}Q = V_l. \tag{1e}$$

Here, $Q(t)$ is the time-dependent (normalized) liquid domain, $\boldsymbol{n} = (0, n_2, n_3)$ is the outer normal, $S(t)$ is the wetted tank surface, and V_l is the nondimensional liquid volume,

$$V_l = \int_{Q(t)} \mathrm{d}Q = \left(\tfrac{1}{2}\pi + z_0\sqrt{1 - z_0^2} + \arcsin(z_0)\right), \tag{2}$$

which should remain constant for the nondimensional mean liquid level z_0 as shown in Fig. 2.1 (a).

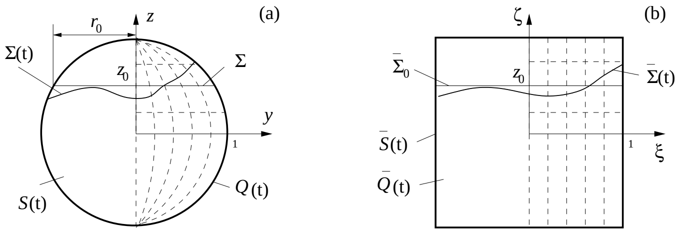

Figure 1: Sketch of a two-dimensional circular tank partly filled by a liquid in the physical plane Oyz (panel a) and its nonconformal transformation to the plane $O\xi\zeta$ (panel b). The figure presents the original liquid volume $Q(t)$, free surface $\Sigma(t)$, the wetted tank walls $S(t)$, and their transformations to the $O\xi\zeta$-plane, $\bar{Q}(t)$, $\bar{\Sigma}(t)$, and $\bar{S}(t)$. The mean free surface Σ_0 corresponds to the vertical liquid level z_0 which remains the same after transformation. The dashed lines show the coordinate curves in physical and transformed planes due to (5).

2.2 Bateman–Luke variational formulation

During the last years, the multimodal method is typically based on the Bateman–Luke variational principle in which the Lagrangian takes the form of the pressure integral. Both the free surface and the velocity potential are two independent parameters and the free surface is implicitly defined by the equation $Z(y,z,t)=0$ [9].

Let us consider an admissible function $\Phi(y,z,t)$ associated with the velocity potential and $Z(y,z,t)$ defining the free surface $\Sigma(t)$ so that the volume conservation condition (1e) is fulfilled for any instant t. According to the Bateman–Luke formulation, the free boundary problem (1) coincides with extrema points of the action

$$A(Z,\Phi)=\int_{t_1}^{t_2} BL(Z,\Phi)\mathrm{d}t$$
$$=-\int_{t_1}^{t_2}\int_{Q(t)}\left[\frac{\partial\Phi}{\partial t}+\tfrac{1}{2}(\nabla\Phi)^2-\frac{\partial\Phi}{\partial y}\dot{\eta}_2+z\right]\mathrm{d}Q\mathrm{d}t \quad (3)$$

for arbitrary t_1 and t_2 ($t_1 < t_2$) and isochronous variations

$$\delta\Phi|_{t_1,t_2} = 0, \quad \delta Z|_{t_1,t_2} = 0. \tag{4}$$

Here, we have employed the nondimensional Bernoulli equation

$$p = -\frac{\partial\Phi}{\partial t} - \tfrac{1}{2}(\nabla\Phi)^2 + \frac{\partial\Phi}{\partial y}\dot{\eta}_2 - z$$

in the non-inertial coordinate system Oyz.

3 Weakly-nonlinear adaptive modal equations

3.1 Nonconformal transformation technique

A way to get a single-valued presentation of the free surface $\Sigma(t)$ can consist of employing the so-called *Lukovsky nonconformal mapping* technique. For the circular tank, this implies transforming the *entire* physical tank domain to a rectangle as it is schematically illustrated in Fig. 2.1. The required transformation between the physical (Oyz) and transformed ($O\xi\zeta$) coordinates may be postulated as

$$y = \xi\sqrt{1-\zeta^2}, \quad z = \zeta; \quad \xi = \frac{y}{\sqrt{1-z^2}}, \quad \zeta = z. \tag{5}$$

The horizontal coordinate curves remain horizontal, but, according to (5), the vertical coordinate lines in the $O\xi\zeta$-plane correspond to the arcs in the physical plane.

In the transformed plane, the free surface $\bar{\Sigma}(t)$ allows for the normal representation

$$\zeta = \tilde{f}(\xi,t) = z_0 + (1-z_0^2)f(\xi,t) = z_0 + r_0^2 f(\xi,t), \tag{6}$$

where function $f(\xi,t)$ defines perturbations of $\bar{\Sigma}(t)$ (and, implicitly, $\Sigma(t)$ in the physical plane) relative to the mean free surface $\bar{\Sigma}_0$ ($z_0 = 0$). Employing (6) and (5) implies that the originally-introduced function Z takes the form

$$Z(y,z,t) = z - z_0 - (1-z_0^2)f\left(\frac{y}{\sqrt{1-z^2}}, t\right), \tag{7}$$

where f is the same as in (6).

Function f should conserve the liquid volume so that (1e) appears as a *holonomic constraint*. Using the Taylor series by f transforms (1e) to

$$\int_{Q(t)} \mathrm{d}Q - V_l = \int_{\bar{Q}(t)} \sqrt{1-\zeta^2}\mathrm{d}Q - V_l$$
$$= \tfrac{1}{2}\int_{-1}^{1}\left[\bar{f}\sqrt{1-\bar{f}^2} + \arcsin\bar{f}\right]\mathrm{d}\xi - z_0\sqrt{1-z_0^2} - \arcsin(z_0)$$
$$= (1-z_0^2)^{3/2}\Bigg[\int_{-1}^{1} f\mathrm{d}\xi - \tfrac{1}{2}z_0\int_{-1}^{1} f^2\mathrm{d}\xi - \tfrac{1}{6}\int_{-1}^{1} f^3\mathrm{d}\xi$$
$$- \tfrac{1}{8}z_0\int_{-1}^{1} f^4\mathrm{d}\xi + O(f^5)\Bigg] = 0. \quad (8)$$

Note that (6) contains the multiplier $r_0^2 = 1 - z_0^2 = (1+z_0)(1-z_0)$ in the front of $f(y,t)$. It has the physical meaning: Because we develop an asymptotic nonlinear modal theory, the smallness of the free surface perturbations should be considered on the three scales, i.e., the free surface length $2r_0$, the maximum liquid depth $1+z_0$ (the free surface does not dry the lower circle pole), and the distance between the mean free surface and the upper liquid pole (there is no overturning). When the tank is about half-filled, all the three scales are of $O(1)$ so that $r_0^2 = O(1)$ and has a symbolic character. In the small depth limit, $(1+z_0) \sim r_0^2 \ll 2r_0$ and, therefore, the free surface perturbation should be smaller that $O(r_0^2)$. Analogously, for the almost filled tank, $(1-z_0) \sim r_0^2 \ll 2r_0$ and, therefore, the free surface perturbation should also be smaller than $O(r_0^2)$.

3.2 Natural sloshing modes

The paper [10] constructed approximate natural sloshing modes, i.e. solutions of the spectral boundary problem in the physical plane

$$\frac{\partial^2\varphi_n}{\partial y^2} + \frac{\partial^2\varphi_i}{\partial z^2} = 0 \text{ in } Q_0; \quad \frac{\partial\varphi_n}{\partial n} = 0 \text{ on } S_0; \quad \frac{\partial\varphi_n}{\partial z} = \kappa_n\varphi_n \text{ on } \Sigma_0, \quad (9)$$

by using the Trefftz variational method with a harmonic basis which satisfies the zero-Neumann boundary condition on the tank surface except in the upper pole:

$$W_i(y,z) = \sum_{k=0}^{[i/2]}(-1)^k C_i^{2k}\left(\frac{2y}{y^2+(z-1)^2}\right)^{i-2k}$$

$$\times \left(-1 - \frac{2(z-1)}{y^2+(z-1)^2}\right)^{2k}, \; i = 0,1,\ldots, \quad (10)$$

where $[i/2]$ is the integer part of $i/2$, and $C_i^{(2k)} = (2k)!/(i!(2k-i)!)$. It has been extensively discussed in [10] that (10) implies a horizontal dipole type flow in the upper circle pole as it was observed in experiments [2].

Following [10], we adopt the following normalized natural sloshing modes

$$\varphi_i(y,z) := \frac{\varphi_i(y,z)}{N_i}, \qquad f_i(y) := \frac{\varphi_i(y,z_0)}{N_i},$$
$$N_i = \operatorname{sign}\left(\varphi_i\left(-r_0, z_0\right)\right) \sqrt{\frac{\int_{-r_0}^{r_0} \varphi_i^2(y,z_0)\mathrm{d}y}{r_0}} \quad (11)$$

providing that the transformed Fourier basis $\bar{f}_n = f_n(\xi r_0) = \varphi_n(\xi r_0, z_0)$ on the mean surface $\bar{\Sigma}_0$ becomes orthogonal, i.e.

$$\int_{-1}^{1} \bar{f}_i \bar{f}_j \mathrm{d}\xi = \delta_{ij}, \quad (12)$$

where δ_{ij} is the Kronecker delta, and the elevation by these functions is positive at the left-side wall.

3.3 Modal solution vs. volume conservation

Now, we are ready to give the needed modal solution in the physical plane. First, we present the velocity potential in the form

$$\Phi(y,z,t) = \dot{\eta}_2(t)y + \sum_{n=1}^{\infty} R_n(t)\varphi_n(y,z), \quad (13)$$

which automatically satisfies the Laplace equation (1a) and the boundary condition (1b) for any admissible position of the free surface $\Sigma(t)$. Furthermore, the free surface is presented by (7) (or by (6) in the transformed plane) where

$$f(\xi,t) = \sum_{i=0}^{\infty} \beta_i(t)\bar{f}_i(\xi) \quad (14)$$

and summation from zero is important to include

$$f_0 = 1/\sqrt{2} \tag{15}$$

which is required to satisfy the volume conservation condition (8) for any instant t.

Substituting the modal solution (14) into the nonlinear volume conservation condition and using the orthogonality condition (12) and expression (15) lead to the equation

$$\begin{aligned}\sqrt{2}\beta_0 = \tfrac{1}{2}z_0\sum_{i=0}^{\infty}\beta_i^2 + \tfrac{1}{6}\sum_{i,j,k=0}^{\infty}\Lambda_{ijk}^{(3)}\beta_i\beta_j\beta_k\\ + \tfrac{1}{8}z_0\sum_{i,j,k,m=0}^{\infty}\Lambda_{ijkm}^{(4)}\beta_i\beta_j\beta_k\beta_m + \ldots,\end{aligned} \tag{16}$$

where the Λ-coefficients are defined in Appendix A.

Considering (16) in a neighborhood of zero (weakly-perturbed free surface), one can resolve it with respect to β_0 rewriting (14) as

$$f(\xi,t) = G(\beta_i) + \sum_{i=1}^{\infty}\beta_i(t)\bar{f}_i(\xi). \tag{17}$$

The function G is found in terms of the Taylor series by $\beta_i(t)$

$$\begin{aligned}G = \frac{1}{4}\Bigg[z_0\sum_{i=1}^{\infty}\beta_i^2 + \tfrac{1}{3}\sum_{i,j,k=1}^{\infty}\Lambda_{ijk}^{(3)}\beta_i\beta_j\beta_k +\\ + \tfrac{1}{4}z_0\left\{\sum_{i,j,k,l=1}^{\infty}\Lambda_{ijkl}^{(4)}\beta_i\beta_j\beta_k\beta_l + (1+\tfrac{1}{2}z_0^2)\left(\sum_{i=1}^{\infty}\beta_i^2\right)^2\right\} + \ldots\Bigg].\end{aligned} \tag{18}$$

In summary, the modal free-surface presentation takes the form

$$\zeta = z_0 + (1-z_0^2)\left[G(\beta_i) + \sum_{i=1}^{\infty}\beta_i(t)\bar{f}_i(\xi)\right], \tag{19a}$$

$$Z(y,z,t) = z - z_0 + (1-z_0^2)\left[G(\beta_i) + \sum_{i=1}^{\infty}\beta_i(t)f_i\left(y\frac{\sqrt{1-z_0^2}}{\sqrt{1-z^2}}\right)\right] =$$

$$= z - z_0 + (1 - z_0^2)\left[G(\beta_i) + \sum_{i=1}^{\infty} \beta_i(t)\varphi_i\left(y\frac{\sqrt{1-z_0^2}}{\sqrt{1-z^2}}, z_0\right)\right], \quad (19b)$$

where function G is given by (18).

3.4 Weakly-nonlinear expressions

The nonconformal mapping technique [15] may adopt the Bateman–Luke variational formulation and the modal solution (13), (19) to be substituted into (3). The result is

$$A(\beta_i, R_n) = -\int_{t_1}^{t_2}\left[\sum_{n=1}^{\infty} A_n \dot{R}_n + \tfrac{1}{2}\sum_{n,k=1}^{\infty} A_{nk} R_n R_k + l_2 \ddot{\eta}_2 + l_3 - \dot{\eta}_2^2\right]\mathrm{d}t, \quad (20)$$

where A_n, A_{nk}, l_2 and l_3 are defined in the physical plane as follows

$$A_n = \int_{Q(t)} \varphi_n \mathrm{d}Q; \quad A_{nk} = \int_{Q(t)} (\nabla\varphi_n \cdot \nabla\varphi_k)\mathrm{d}Q,$$
$$l_2 = \int_{Q(t)} y\mathrm{d}Q; \quad l_3 = \int_{Q(t)} z\mathrm{d}Q. \quad (21)$$

Derivation of the kinematic and dynamic modal equations suggests variation by independent generalized coordinates β_i and velocities R_n and equating the result to zero. The obtained variational equations should be considered together with condition (4) which means that

$$\delta\beta_i(t_1) = \delta\beta_i(t_2) = \delta R_n(t_1) = \delta R_n(t_2) = 0. \quad (22)$$

During this derivation, it is important that expressions (21) can be explicitly presented in term of the generalized coordinates β_i:

$$A_n = \int_{-1}^{1} \int_{-1}^{z_0 + (1-z_0^2)\left[G(\beta_i) + \sum_{i=1}^{\infty} \beta_i \bar{f}_i\right]} \varphi_n\left(\xi\sqrt{1-\zeta^2}, \zeta\right)\sqrt{1-\zeta^2}\,\mathrm{d}\zeta\mathrm{d}\xi, \quad (23a)$$

$$A_{nk} = \int_{-1}^{1} \int_{-1}^{z_0 + (1-z_0^2)\left[G(\beta_i) + \sum_{i=1}^{\infty} \beta_i \bar{f}_i\right]} \left[\left(\frac{\partial\varphi_n}{\partial y}\right)^2 + \left(\frac{\partial\varphi_n}{\partial z}\right)^2\right]_{y=\xi\sqrt{1-\zeta^2}, z=\zeta}$$

$$\times \sqrt{1-\zeta^2}\ \mathrm{d}\zeta\mathrm{d}\xi, \quad (23b)$$

$$l_2 = \int_{-1}^{1}\int_{-1}^{z_0+(1-z_0^2)\left[G(\beta_i)+\sum\limits_{i=1}^{\infty}\beta_i\bar{f}_i\right]} \xi(1-\zeta^2)\ \mathrm{d}\zeta\mathrm{d}\xi, \qquad (23c)$$

$$l_3 = \int_{-1}^{1}\int_{-1}^{z_0+(1-z_0^2)\left[G(\beta_i)+\sum\limits_{i=1}^{\infty}\beta_i\bar{f}_i\right]} \zeta\sqrt{1-\zeta^2}\ \mathrm{d}\zeta\mathrm{d}\xi. \qquad (23d)$$

3.4.1 Kinematic modal equations

To get the kinematic modal equations, we vary functional (20) by independent generalized velocities $R_n, n \geq 1$ and equal it to zero. Analogously to derivations in [9], the latter equality will, after integrating by part and using condition (22), lead to

$$\frac{dA_n}{dt} = \sum_{k=1}^{\infty} A_{nk}R_k, \quad n \geq 1. \qquad (24)$$

Here, according to definitions (23a),

$$\frac{dA_n}{dt} = \sum_{k=1}^{\infty} \frac{\partial A_n}{\partial \beta_k}\dot{\beta}_k, \qquad (25)$$

and

$$\frac{\partial A_n}{\partial \beta_k} = (1-z_0^2)\int_{-1}^{1}\left[\varphi_n\left(\xi\sqrt{1-\zeta^2},\zeta\right)\sqrt{1-\zeta^2}\right]_{\zeta=z_0+(1-z_0^2)\left[G(\beta_i)+\sum\limits_{i=1}^{\infty}\beta_i\bar{f}_i\right]} \times\left[\bar{f}_k+\frac{\partial G}{\partial \beta_k}\right]\mathrm{d}\xi.$$

Keeping the quadratic terms gives

$$\frac{\partial A_n}{\partial \beta_k} = r_0^3\left[\delta_{nk}+\sum_{i=1}^{\infty}\chi^{(1)}_{n,k,i}\beta_i+\sum_{i,j=1}^{\infty}\chi^{(2)}_{n,k,i,j}\beta_i\beta_j\right], \qquad (26a)$$

$$A_{nk} = r_0\left[\kappa_n\delta_{nk}+\sum_{i=1}^{\infty}\Pi^{(1)}_{nk,i}\beta_i+\tfrac{1}{2}\sum_{i,j=1}^{\infty}\Pi^{(2)}_{nk,ij}\beta_i\beta_j\right], \qquad (26b)$$

where

$$\begin{aligned}
\chi^{(1)}_{n,k,i} &= (\kappa_n r_0^2 - z_0)\Lambda^{(3)}_{nki} - z_0\Lambda^{(3,1,\xi)}_{n,ki},\\
\chi^{(2)}_{n,k,i,j} &= (-\tfrac{1}{2} - z_0\kappa_n r_0^2)\Lambda^{(4)}_{nkij} + (z_0^2 - \tfrac{1}{2} - \kappa_n z_0 r_0^2)\Lambda^{(4,1,\xi)}_{n,kij} + \tfrac{1}{2}z_0^2\Lambda^{(4,2,\xi^2)}_{n,kij}\\
&\quad - \tfrac{1}{2}r_0^2\Lambda^{(4,2)}_{n,kij} + \tfrac{1}{2}z_0(\kappa_n r_0^2 - z_0)(\delta_{ni}\delta_{jk} + \tfrac{1}{2}\delta_{ij}\delta_{nk})\\
&\quad - \tfrac{1}{2}z_0^2\left(\delta_{jk}\Lambda^{(2,1,\xi)}_{n,i} + \tfrac{1}{2}\delta_{ij}\Lambda^{(2,1,\xi)}_{n,k}\right),\\
\Pi^{(1)}_{nk,i} &= r_0^2\kappa_n\kappa_k\Lambda^{(3)}_{nki} + \Lambda^{(3,1,1)}_{nk,i},\\
\Pi^{(2)}_{nk,ij} &= -z_0\kappa_n\kappa_k r_0^2\left(\Lambda^{(4)}_{nkij} + \Lambda^{(4,1,\xi)}_{k,nij} + \Lambda^{(4,1,\xi)}_{n,kij}\right)\\
&\quad + \left(r_0^2(\kappa_n + \kappa_k) - z_0\right)\Lambda^{(4,1,1)}_{nk,ij} - r_0^2\left[\kappa_n\Lambda^{(4,2)}_{k,nij} + \kappa_k\Lambda^{(4,2)}_{n,kij}\right]\\
&\quad - z_0\left[\Lambda^{(4,2,1,\xi)}_{n,k,ij} + \Lambda^{(4,2,1,\xi)}_{k,n,ij}\right] + \tfrac{1}{4}z_0\delta_{ij}\left[r_0^2\kappa_n\kappa_k\delta_{nk} + \Lambda^{(2,1,1)}_{nk}\right]
\end{aligned}$$

and the Λ-coefficients are defined in Appendix A.

Now we can consider the kinematic modal equations (24), (25) with expressions (26a) and (26b) as a system of linear algebraic equations with respect to R_n. For this purpose, we present the generalized coordinates

$$R_k = r_0^2\left[\frac{\dot\beta_k}{\kappa_k} + \sum_{p,q=1}^{\infty} V^{(2)}_{k,p,q}\dot\beta_p\beta_q + \sum_{p,q,l=1}^{\infty} V^{(3)}_{k,p,q,l}\dot\beta_p\beta_q\beta_l\right] \tag{27}$$

and substitute (27) into the kinematic modal equations (24) to find that

$$V^{(2)}_{n,p,q} = \frac{1}{\kappa_n}\left[\chi^{(1)}_{n,p,q} - \frac{\Pi^{(1)}_{np,q}}{\kappa_p}\right],$$

$$V^{(3)}_{n,p,q,l} = \frac{1}{\kappa_n}\left[\chi^{(2)}_{n,p,q,l} - \frac{\Pi^{(2)}_{np,ql}}{2\kappa_p} - \sum_{k=1}^{\infty} V^{(2)}_{k,p,q}\Pi^{(1)}_{nk,l}\right].$$

Here the inner summation by k is infinite that is in contrast to the analogous expressions in [8] for a rectangular tank where the trigonometric natural modes provided zeros of Λ-coefficients when one of the indexes tends to infinity.

In summary, the kinematic modal equations gave us asymptotic solution (27) in terms of the generalized coordinates R_k with respect to another set of generalized coordinates β_k by (27), where the V-coefficients are known functions of z_0.

3.4.2 Dynamic modal equations

To derive the dynamic modal equations, we should vary the functional (20) by independent generalized coordinates $\beta_\mu, \mu \geq 1$ and equal the result to zero. The leads to the equalities

$$\sum_{n=1}^{\infty} \frac{\partial A_n}{\partial \beta_\mu} \dot{R}_n + \frac{1}{2} \sum_{n,k=1}^{\infty} \frac{\partial A_{nk}}{\partial \beta_m} R_n R_k + \frac{\partial l_2}{\partial \beta_\mu} \ddot{\eta}_2 + \frac{\partial l_3}{\partial \beta_\mu} = 0, \quad \mu \geq 1. \tag{28}$$

Looking for a weakly-nonlinear solution, we should, according to (26b), use the expressions

$$\frac{\partial A_{nk}}{\partial \beta_\mu} = r_0 \left[\Pi^{(1)}_{nk,\mu} + \sum_{j=1}^{\infty} \Pi^{(2)}_{nk,\mu j} \beta_j \right], \tag{29}$$

(26a) (for $\partial A_n / \partial \beta_\mu$), and R_n are, due to (27), equal to

$$\dot{R}_k = r_0^2 \left[\frac{\ddot{\beta}_k}{\kappa_k} + \sum_{p,q=1}^{\infty} V^{(2)}_{k,p,q} \ddot{\beta}_p \beta_q + \sum_{p,q,l=1}^{\infty} V^{(3)}_{k,p,q,l} \ddot{\beta}_p \beta_q \beta_l + \sum_{p,q=1}^{\infty} V^{(2)}_{k,p,q} \dot{\beta}_p \dot{\beta}_q + \right.$$
$$\left. + \sum_{p,q,l=1}^{\infty} \bar{V}^{(3)}_{k,pq,l} \dot{\beta}_p \dot{\beta}_q \beta_l \right], \quad \bar{V}^{(3)}_{k,pq,l} = V^{(3)}_{k,p,q,l} + V^{(3)}_{k,p,l,q}. \tag{30}$$

Furthermore, we should take care of $\partial l_2 / \partial \beta_\mu$ and $\partial l_3 / \partial \beta_\mu$ defined by (23c) and (23d), respectively.

For the asymptotic modal equations, the quantity $\partial l_2 / \partial \beta_\mu$ appears at the excitation term which is of the highest order in our asymptotic modal analysis. Thus, we need only to account for the lowest order term, $O(1)$, which is computed as

$$\frac{\partial l_2}{\partial \beta_\mu} = r_0^4 \int_{-1}^{1} \xi \bar{f}_\mu \mathrm{d}\xi + O(\beta) = r_0^4 \lambda_{2\mu} + O(\beta). \tag{31}$$

Another term is generally defined by the formula

$$\frac{\partial l_3}{\partial \beta_\mu} = r_0^2 \int_{-1}^{1} \zeta \sqrt{1-\zeta^2} |_{\zeta = z_0 + (1-z_0^2)\left[G(\beta_i) + \sum_{i=1}^{\infty} \beta_i \bar{f}_i\right]} \left[f_\mu + \frac{\partial G}{\partial \beta_\mu} \right] \mathrm{d}\xi \tag{32}$$

which should be expanded in a Taylor series by generalized coordinates

$$\frac{\partial l_3}{\partial \beta_\mu} = r_0^5 \left[\beta_\mu - z_0 \sum_{i,j=1}^{\infty} \Lambda^{(3)}_{ij\mu} \beta_i \beta_j - \frac{1}{2} \sum_{i,j,k=1}^{\infty} \Lambda^{(4)}_{ijk\mu} \beta_i \beta_j \beta_k - \frac{3}{4} z_0^2 \beta_\mu \sum_{i=1}^{\infty} \beta_i^2 \right]. \tag{33}$$

3.4.3 Adaptive modal equations

Including up to the third-order polynomial quantities in the dynamic equations (28) leads to

$$\sum_{k=1}^{\infty}\ddot{\beta}_k\left[\delta_{k\mu}+\sum_{i=1}^{\infty}d^{(1)}_{\mu,k,i}\beta_i+\sum_{i,j=1}^{\infty}d^{(2)}_{\mu,k,i,j}\beta_i\beta_j\right]$$
$$+\sum_{p,q=1}^{\infty}\dot{\beta}_p\dot{\beta}_q\left[t^{(0)}_{\mu,p,q}+\sum_{i=1}^{\infty}t^{(2)}_{\mu,p,p,i}\beta_i\right]+\kappa_\mu\beta_\mu+\sum_{i,j=1}^{\infty}g^{(2)}_{\mu,ij}\beta_i\beta_j$$
$$+\sum_{i,j,k=1}^{\infty}g^{(3)}_{\mu,ij,k}\beta_i\beta_j\beta_k+\kappa_\mu\lambda_{2\mu}\frac{\ddot{\eta}_2}{r_0}=0,\quad \mu\geq 1, \tag{34}$$

where

$$d^{(1)}_{\mu,k,i}=\kappa_\mu\left[V^{(2)}_{\mu,k,i}+\frac{\chi^{(1)}_{k,\mu,i}}{\kappa_k}\right], \tag{35a}$$

$$d^{(2)}_{\mu,k,i,j}=\kappa_\mu\left[V^{(3)}_{\mu,k,i,j}+\frac{\chi^{(2)}_{k,\mu,i,j}}{\kappa_k}+\sum_{l=1}^{\infty}\chi^{(1)}_{l,\mu,i}V^{(2)}_{l,k,j}\right], \tag{35b}$$

$$t^{(0)}_{\mu,p,q}=\kappa_\mu\left[V^{(2)}_{\mu,p,q}+\frac{\Pi^{(1)}_{pq,\mu}}{2\kappa_p\kappa_q}\right], \tag{35c}$$

$$t^{(1)}_{\mu,p,q,i}=\kappa_\mu\left[\bar{V}^{(3)}_{\mu,p,q,i}+\frac{\Pi^{(2)}_{pq,i\mu}}{2\kappa_p\kappa_q}+\sum_{k=1}^{\infty}V^{(2)}_{k,p,q}\chi^{(1)}_{k,\mu,i}+\sum_{k=1}^{\infty}\frac{\Pi^{(1)}_{kq,\mu}V^{(2)}_{k,p,i}}{\kappa_q}\right], \tag{35d}$$

$$g^{(2)}_{\mu,ij}=-z_0\kappa_\mu\Lambda^{(3)}_{ij\mu}, \tag{35e}$$

$$g^{(3)}_{\mu,ij,k}=-\kappa_\mu\left[\tfrac{1}{2}\Lambda^{(4)}_{ijk\mu}+\tfrac{3}{4}z_0^2\delta_{ij}\delta_{k\mu}\right]. \tag{35f}$$

Here, the inner summations in the hydrodynamic coefficients are indeed infinite. Furthermore, since β_{2k-1} correspond to antisymmetric modes, but β_{2k} are generalized coordinates responsible for symmetric modes, the hydrodynamic coefficients possess the properties

$$\begin{aligned}&d^{(1)}_{\mu,i,j}=t^{(0)}_{\mu,i,j}=g^{(2)}_{\mu,i,j}=0, \qquad \bmod\,(\mu+i+j,2)=1,\\ &d^{(2)}_{\mu,i,j,k}=t^{(0)}_{\mu,i,j,k}=g^{(2)}_{\mu,i,j,k}=0, \qquad \bmod\,(\mu+i+j+k,2)=1,\end{aligned} \tag{36}$$

which leads to specific zeros in (53).

The novelty of these equations with respect to those for cylindrical tanks [8] is additional nonlinear terms associated with the g-coefficients caused by the fact that the vertical coordinate lines in the transformed plane are not along the gravity acceleration vector.

3.4.4 Horizontal hydrodynamic force

According to Lukovsky's formula [9] the hydrodynamic force is determined by the mass center motions so that the dimensional horizontal force is

$$F_2(t) = m_l g(\ddot{\eta}_2 + \ddot{y}_C(t)), \tag{37}$$

where the horizontal component of the mass centre is defined by l_2 and can, within the framework of the third-order approximation, be computed by the formula

$$y_C(t)\, V_l = l_2 = r_0^4 \left[\sum_{i=1}^{\infty} \lambda_{2i}\beta_i \left(1 - \tfrac{1}{2} z_0^2 \sum_{j=1}^{\infty} \beta_j^2 \right) - z_0 \sum_{i,j=1}^{\infty} \lambda_{2ij}\beta_i\beta_j - \right.$$
$$\left. - r_0^2 \sum_{i,j,k=1}^{\infty} \lambda_{2ijk}\beta_i\beta_j\beta_k \right], \tag{38}$$

where the λ-coefficients are defined by (52). We can see that, in contrast to, e.g., rectangular tank [8], $y_C(t)$ component of the mass centre is strongly nonlinearly dependent on the generalized coordinates.

Accounting for expression (38), the horizontal force takes the form

$$F_2(t) = m_l g \left(\ddot{\eta}_2 + \frac{r_0^4}{V_l} \left[\sum_{i=1}^{\infty} \ddot{\beta}_i \left\{ f_{0i} + \sum_{j=1}^{\infty} f_{1ij}\beta_j + \sum_{j,k=1}^{\infty} f_{2i,j,k}\beta_j\beta_k \right\} \right.\right.$$
$$\left.\left. + \sum_{i,j=1}^{\infty} \dot{\beta}_i\dot{\beta}_j \left\{ h_{0ij} + \sum_{k=1}^{\infty} h_{1i,j,k}\beta_k \right\} \right] \right), \tag{39}$$

where

$$f_{0i} = \lambda_{2i};\; f_{1ij} = -2z_0\lambda_{2ij};\; f_{2i,j,k} = -z_0^2 \left(\tfrac{1}{2}\lambda_{2i}\delta_{jk} + \lambda_{2j}\delta_{ik} \right) - 3r_0^2\lambda_{2ijk}, \tag{40a}$$
$$h_{0ij} = -2z_0\lambda_{2ij};\;\; h_{1i,j,k} = -z_0^2 \left(2\lambda_{2i}\delta_{jk} + \lambda_{2k}\delta_{ij} \right) - 6r_0^2\lambda_{2ijk}. \tag{40b}$$

Here, we also have many zeros due to the property

$$\begin{aligned} f_{0i} = 0, \quad \bmod\ (i,2) = 0;\ f_{1ij} = h_{0ij} = 0, \quad \bmod\ (i+j,2) = 0, \\ f_{2i,j,k} = h_{1i,j,k} = 0 \quad \bmod\ (i+j+k,2) = 0. \end{aligned} \tag{41}$$

4 Narimanov–Moiseev modal equations

The Narimanov–Moiseev theory is based on the Duffing asymptotic ordering [9] assuming that the primary-excited first mode is the only dominant and of the order $\beta_1 = O(\epsilon^{1/3})$ when the forcing is of the order $\eta_2 = O(\epsilon), \epsilon \ll 1$. The non-zero second-order polynomial terms in β_1 appear for the circular tank shape in all modal equations (34) responsible for symmetric modes while the nonzero cubic terms in β_1 exist in all modal equations (34) governing the antisymmetric modes. This means that the Narimanov–Moiseev asymptotics takes in the studied case the form

$$\beta_1 = O(\epsilon^{1/3}), \quad \beta_{2k} = O(\epsilon^{2/3}), \quad \beta_{2k+1} = O(\epsilon), \quad k \geq 1. \tag{42}$$

Neglecting the $o(\epsilon)$-terms in (34) and using the generalized Moiseev asymptotics (42), we arrive at the following Narimanov–Moiseev system of modal equations

$$\begin{aligned} &\ddot{\beta}_{2\mu-1} + \kappa_{2\mu-1}\beta_{2\mu-1} + d^{(2)}_{2\mu-1,1,1,1}\ddot{\beta}_1\beta_1^2 + t^{(1)}_{2\mu-1,1,1,1}\dot{\beta}_1^2\beta_1 \\ &\quad + g^{(3)}_{2\mu-1,1,1,1}\beta_1^3 + \ddot{\beta}_1\sum_{i=1}^{\infty} d^{(1)}_{2\mu-1,1,2i}\beta_{2i} + \beta_1\sum_{i=1}^{\infty} d^{(1)}_{2\mu-1,2i,1}\ddot{\beta}_{2i} \\ &\quad + \dot{\beta}_1\sum_{i=1}^{\infty}\left[t^{(0)}_{2\mu-1,1,2i} + t^{(0)}_{2\mu-1,2i,1}\right]\dot{\beta}_{2i} + 2\beta_1\sum_{i=1}^{\infty} g^{(2)}_{(2\mu-1)1(2i)}\beta_{2i} \\ &\quad + \kappa_{2\mu-1}\lambda_{2(2\mu-1)}\frac{\ddot{\eta}_2}{r_0} = 0, \end{aligned} \tag{43a}$$

$$\ddot{\beta}_{2\mu} + \kappa_{2\mu}\beta_{2\mu} + d^{(1)}_{2\mu,1,1}\ddot{\beta}_1\beta_1 + t^{(0)}_{2\mu,1,1}\dot{\beta}_1 = 0, \quad \mu = 1, \ldots. \tag{43b}$$

Referring to numerical simulation and experimental data [10] commented on the possibility of the *internal (secondary) resonance* which causes both amplification of higher modes and transition to three-dimensional flow [3, 20]. The secondary resonance may make the modal

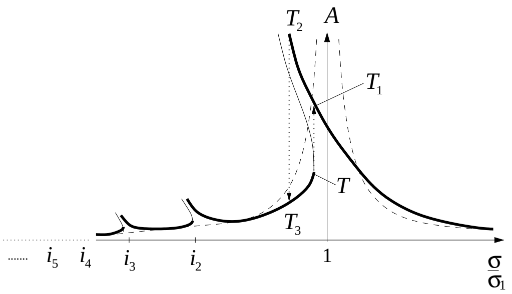

Figure 2: The schematic response curves for a clean rectangular tank representing the maximum steady-state wave elevation A versus σ/σ_1 for $0.3368\ldots < h/l$ due to lateral harmonic excitation. The dashed line shows results of the linear sloshing theory. The solid bold lines display stable nonlinear steady-state regimes. A hysteresis effect at $\sigma/\sigma_1 = 1$ is possible and denoted by the points T, T_1, T_2 and T_3. The points i_2 and i_3 mark the most important secondary resonance points occurring when the forcing frequency satisfies the conditions $2\sigma = \sigma_2$ (amplification of the second mode) or $3\sigma = \sigma_3$ (amplification of the third mode), respectively. A hysteresis effect at i_2 and i_3 is also possible but, due to sufficiently large damping, it was detected in experiments [8] only for a relatively-large forcing amplitude.

system (43) inapplicable. Papers [8,12,19] presented a detailed theoretical and experimental analysis of the *secondary-resonance phenomena* for liquid sloshing dynamics. An extended review on the secondary resonance phenomenon for two-dimensional and three-dimensional sloshing is also given in Chapt. 8 of [9]. In these publications, the phenomena are studied for the case when the tank is harmonically forced, horizontally or angularly, with an asymptotically-small amplitude and the forcing frequency σ is close to the lowest natural sloshing frequency σ_1, i.e. $\sigma \approx \sigma_1$. The primary emphasis is placed on the two-dimensional steady-state resonant liquid sloshing in a clean rectangular tank for which the secondary resonance phenomenon is expected at $2\sigma \approx \sigma_2$, $3\sigma \approx \sigma_3$,..., $n\sigma \approx \sigma_n, n \geq 4$. The latter conditions imply amplification of the second, third, and higher harmonics as well as the corresponding natural modes. Thinking in terms of the multimodal method, the harmonics are mathematically yielded by the free-surface nonlinearities of the corresponding polynomial orders. For $0.3368\ldots < h/l$ ($0.3368\ldots$ is the so-called critical depth where the soft-to-hard spring behavior of the response curves changes with $\sigma = \sigma_1$, h is the rectangular tank depth, and l is the tank width), the secondary resonance peaks on the steady-state response curves are situated away from the primary resonance $\sigma = \sigma_1$ as shown in Fig. 4. Passage to shallow water depths moves the points i_k closer to 1 and, thereby, increases the probability of the secondary resonance for higher modes. However, the liquid damping causes that the secondary resonance peaks associated with higher-order free-surface nonlinearities (fourth, fifth, etc.) remain quite narrow and they are practically realized only for nearly-shallow water conditions with $h/l \lesssim 0.2$.

Specific position of the secondary resonance peaks in Fig. 4 and, therefore, contribution of higher modes is only typical to rectangular tanks. The secondary resonance peaks may change positions for other tank shape and even, as it is shown in [6, 7] due to internal structures installed in the tank. This fact was extensively discussed in [7] in the context of nonlinear liquid sloshing with a central slotted screen installed at the rectangular tank by employing the 'modal equations' language. For the modal equations (34) derived for circular tank, the calculations show that the nonzero quadratic quantities in β_1 appear now in all the equations for even modes, i.e. all the symmetric modes (associated with β_{2i}) can be amplified due to the second harmonics (the second-order nonlinearity) but the nonzero cubic terms in β_1 are present in all the equations for antisymmetric modes (associated with β_{2i-1}). As a consequence, the higher solidity ratios yield the secondary resonance due to the second and third harmonics not only at i_2 and i_3 but also at i_k, $k \geq 2$ defined by

$$2\sigma = \sigma_{2k} \quad \Longrightarrow \quad \frac{\sigma}{\sigma_1} = \frac{\sigma_{2k}}{2\sigma_1} = i_{2k}, \qquad k = 1, 2, \ldots \tag{44}$$

(due to amplification of the double harmonics) and

$$3\sigma = \sigma_{2k+1} \quad \Longrightarrow \quad \frac{\sigma}{\sigma_1} = \frac{\sigma_{2k+1}}{3\sigma_1} = i_{2k+1}, \qquad k = 1, 2, \ldots . \tag{45}$$

(due to amplification of the third harmonics).

Occurrence of the secondary resonance due to excitation of the first sloshing mode is expected when $\sigma/\sigma_1 \approx 1$ and $\sigma/\sigma_1 \approx i_m$ for a certain indexes m, simultaneously. Fig. 4 shows that this really can happen for different liquid depths. So, Fig. 4 (a) demonstrates that amplification of the double harmonics due to quadratic terms in the equations for the

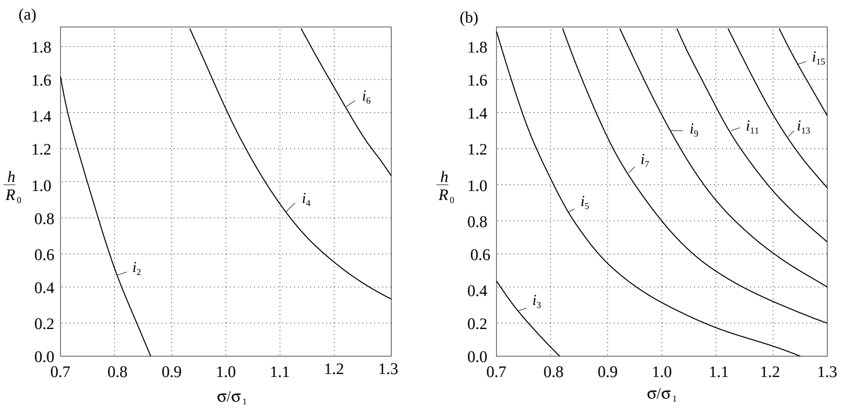

Figure 3: Occurrence of the secondary resonance due to the second harmonics $i_{2k} \approx 1$ and the third harmonics $i_{2k+1} \approx 1, k = 1, \ldots$ for different liquid depths and the forcing frequency close to the lowest natural frequency.

symmetric modes is, first of all, dangerous for the fourth mode. According to Fig. 4 (b), the harmonics 3σ will primary cause amplification of the fifth and seventh modes for lower depths, but the ninth and eleventh mode amplification is expected for higher liquid depths.

5 Concluding remarks

The paper opens a series of analytical studies on nonlinear liquid sloshing in a two-dimensional circular tank. The literature on that is almost empty and the theoretical papers are normally based on the linear statement, or perform direct simulations employing CFD. In the present paper, we derive the so-called adaptive and Narimanov–Moiseev weakly-nonlinear modal equations. According to the secondary resonance analysis, the Narimanov–Moiseev modal equations may have a limited applicability, especially for higher tank fillings. This needs a dedicated study what should employ a comparison with experiments.

A Definitions of coefficients

$$\Lambda^{(3)}_{ijk} = \int_{-1}^{1} \bar{f}_i \bar{f}_j \bar{f}_k \mathrm{d}\xi, \quad \Lambda^{(4)}_{ijkm} = \int_{-1}^{1} \bar{f}_i \bar{f}_j \bar{f}_k \bar{f}_m \mathrm{d}\xi, \ldots, \tag{46}$$

$$\Lambda^{(2,1,\xi)}_{n,k} = \int_{-1}^{1} \xi \bar{f}_{n\xi} \bar{f}_k \mathrm{d}\xi, \quad \Lambda^{(3,1,\xi)}_{n,ki} = \int_{-1}^{1} \xi \bar{f}_{n\xi} \bar{f}_k \bar{f}_i \mathrm{d}\xi,$$
$$\Lambda^{(4,1,\xi)}_{n,kij} = \int_{-1}^{1} \xi \bar{f}_{n\xi} \bar{f}_k \bar{f}_i \bar{f}_j \mathrm{d}\xi, \ldots, \quad (47)$$

$$\Lambda^{(2,1,1)}_{nk} = \int_{-1}^{1} \bar{f}_{n\xi} \bar{f}_{k\xi} \mathrm{d}\xi, \quad \Lambda^{(3,1,1)}_{nk,i} = \int_{-1}^{1} \bar{f}_{n\xi} \bar{f}_{k\xi} \bar{f}_i \mathrm{d}\xi,$$
$$\Lambda^{(4,1,1)}_{n,ki} = \int_{-1}^{1} \bar{f}_{n\xi} \bar{f}_{k\xi} \bar{f}_i \bar{f}_j \mathrm{d}\xi, \ldots, \quad (48)$$

$$\Lambda^{(3,2)}_{n,ij} = \int_{-1}^{1} \bar{f}_{n\xi\xi} \bar{f}_i \bar{f}_j \mathrm{d}\xi, \quad \Lambda^{(4,2)}_{n,ijl} = \int_{-1}^{1} \bar{f}_{n\xi\xi} \bar{f}_i \bar{f}_j \bar{f}_l \mathrm{d}\xi, \ldots, \quad (49)$$

$$\Lambda^{(3,2,\xi^2)}_{n,ij} = \int_{-1}^{1} \xi^2 \bar{f}_{n\xi\xi} \bar{f}_i \bar{f}_j \mathrm{d}\xi, \quad \Lambda^{(4,2,\xi^2)}_{n,ijl} = \int_{-1}^{1} \xi^2 \bar{f}_{n\xi\xi} \bar{f}_i \bar{f}_j \bar{f}_l \mathrm{d}\xi, \ldots, \quad (50)$$

$$\Lambda^{(3,2,1,\xi)}_{n,k,i} = \int_{-1}^{1} \xi \bar{f}_{n\xi\xi} \bar{f}_{k\xi} \bar{f}_i \mathrm{d}\xi, \quad \Lambda^{(4,2,1,\xi)}_{n,i,jl} = \int_{-1}^{1} \xi \bar{f}_{n\xi\xi} \bar{f}_{k\xi} \bar{f}_i \bar{f}_j \mathrm{d}\xi, \ldots, \quad (51)$$

$$\lambda_{2n} = \int_{-1}^{1} \xi \bar{f}_n \mathrm{d}\xi, \quad \lambda_{2nk} = \int_{-1}^{1} \xi \bar{f}_n \bar{f}_k \mathrm{d}\xi, \quad \lambda_{2nki} = \int_{-1}^{1} \xi \bar{f}_n \bar{f}_k \bar{f}_i \mathrm{d}\xi, \ldots. \quad (52)$$

B Modal expressions adopted for calculations

It is convenient for calculation to rewrite the truncated nonlinear modal equations (34) in the form

$$\sum_{a=1}^{N} \ddot{\beta}_a \left(\delta_{am} + \sum_{b=1}^{N} \beta_b D1^m(a,b) + \sum_{b=1}^{N} \sum_{c=1}^{b} D2^m(a,b,c) \beta_b \beta_c \right)$$
$$+ \sum_{a=1}^{N} \sum_{b=1}^{a} \dot{\beta}_a \dot{\beta}_b \left(T0^m(a,b) + \sum_{c=1}^{N} T1^m(a,b,c) \beta_c \right) + \kappa_m \beta_m$$
$$+ \sum_{a=1}^{N} \sum_{b=1}^{a} G2^m(a,b) \beta_a \beta_b + \sum_{a=1}^{N} \sum_{b=1}^{a} \sum_{c=1}^{b} G3^m(a,b,c) \beta_a \beta_b \beta_c + P_m \ddot{\eta}_2 = 0, \quad (53)$$

where

$$P_m = \kappa_m \frac{\lambda_{2m}}{r_0}; \quad D1^m(a,b) = d^{(1)}_{m,a,b},$$

$$D2^m(a,b,c) = \begin{cases} d^{(2)}_{m,a,b,b}, & b = c, \\ d^{(2)}_{m,a,b,c} + d^{(2)}_{m,a,c,b}, & b \neq c, \end{cases}$$

$$T0^m(a,b) = \begin{cases} t^{(0)}_{m,a,a}, & a = b, \\ t^{(0)}_{m,a,b} + t^{(0)}_{m,b,a}, & a \neq b; \end{cases}$$

$$T1^m(a,b,c) = \begin{cases} t^{(1)}_{m,a,a,c}, & a = b, \\ t^{(1)}_{m,a,b,c} + t^{(1)}_{m,b,a,c}, & a \neq b, \end{cases}$$

$$G2^m(a,b) = \begin{cases} g^{(2)}_{m,a,a}, & a = b, \\ g^{(2)}_{m,a,b} + g^{(2)}_{m,b,a}, & a \neq b, \end{cases}$$

$$G3^m(b,c,d) = \begin{cases} g^{(3)}_{m,b,b,b}, & b = c = d, \\ g^{(3)}_{m,b,b,d} + g^{(3)}_{m,b,d,b} + g^{(3)}_{m,d,b,b}, & b = c,\ c \neq d, \\ g^{(3)}_{m,b,c,c} + g^{(3)}_{m,c,b,c} + g^{(3)}_{m,c,c,b}, & b \neq c,\ c = d, \\ g^{(3)}_{m,b,c,d} + g^{(3)}_{m,b,d,c} + g^{(3)}_{m,c,b,d} & \\ +g^{(3)}_{m,c,d,b} + g^{(3)}_{m,d,b,c} + g^{(3)}_{m,d,c,b}, & b \neq c,\ c \neq d. \end{cases}$$

The force is due to (39) presented for calculations by the truncated formula

$$F_2(t) = m_l g\Big(\ddot{\eta}_2 + \frac{r_0^4}{V_l}\Big[\sum_{i=1}^{N} \ddot{\beta}_i \Big\{F_0(i) + \sum_{j=1}^{N} F_1(i,j)\beta_j + \sum_{j=1}^{N}\sum_{k=1}^{j} F_2(i,j,k)\beta_j\beta_k\Big\}$$
$$+ \sum_{i=1}^{N}\sum_{j=1}^{i} \dot{\beta}_i\dot{\beta}_j \Big\{H_0(i,j) + \sum_{k=1}^{N} H_1(i,j,k)\beta_k\Big\}\Big]\Big), \qquad (54)$$

where

$$F_0(i) = f_{0i}; \quad F_1(i,j) = f_{1ij}; \quad F_2(i,j,k) = \begin{cases} f_{2,i,j,j}, & j = k, \\ f_{2,i,j,k} + f_{2,i,k,j}, & j \neq k, \end{cases}$$

$$H_0(i,j) = \begin{cases} h_{0ii}, & i = j, \\ 2h_{0ij}, & i \neq j; \end{cases} \qquad H_1(i,j,k) = \begin{cases} h_{1,i,i,k}, & i = j, \\ h_{1,i,j,k} + h_{1,j,i,k}, & i \neq j. \end{cases}$$

[1] *Aliabadi S., Johnson A., Abedi J.* Comparison of finite element and pendulum models for simulating of sloshing // Computers and Fluids. — 2003. — **32**. — P. 535–545.

[2] *Barkowiak K., Gampert B., Siekmann J.* On liquid motion in a circular cylinder with horizontal axis // Acta Mechanica. — 1985. — **54**. — P. 207–220.

[3] *Bogomaz G.I., Sirota S.A.* Oscillations of a liquid in containers: Methods and results of experimental studies. — Dnepropetrovsk: National Space Agency of Ukraine, 2002 (in Russian). — 160 p.

[4] *Djavareshkian M.H., Khalili M.* Simulation of sloshing with the Volume of Fluid Method // Fluid Dynamics and Materials Processing. — 2006. — **2**, No. 4. — P. 299–307.

[5] *Eastham M.* An eigenvalue problem with parameter in the boundary condition // Quarterly J. of Mathematics. — 1962. — **13**. — P. 304–320.

[6] *Faltinsen O.M., Firoozkoohi R., Timokha A.N.* Steady-state liquid sloshing in a rectangular tank with a slat-type screen in the middle: quasi-linear modal analysis and experiments // Physics of Fluids. — 2011. — **23**, Art. No. 042101.

[7] *Faltinsen O.M., Firoozkoohi R., Timokha A.N.* Effect of central slotted screen with a high solidity ratio on the secondary resonance phenomenon for liquid sloshing in a rectangular tank // Physics of Fluids. — 2011. — **23**, Art. No. 062106.

[8] *Faltinsen O.M., Timokha A.N.* Adaptive multimodal approach to nonlinear sloshing in a rectangular tank // J. of Fluid Mechanics. — 2001. — **432**. — P. 167–200.

[9] *Faltinsen O.M., Timokha A.N.* Sloshing. — Cambridge: Cambridge University Press, 2009. — 680 p.

[10] *Faltinsen O.M., Timokha A.N.* A multimodal method for liquid sloshing in a two-dimensional circular tank // J. of Fluid Mechanics. — 2010. — **665**. — P. 457–479.

[11] *Faltinsen O.M., Timokha A.N.* On sloshing modes in a circular tank // J. of Fluid Mechanics. — 2012. — **695**. — P. 467-477.

[12] *Hermann M., Timokha A.* Modal modelling of the nonlinear resonant fluid sloshing in a rectangular tank II: Secondary resonance // Mathematical Models and Methods in Applied Sciences. — 2008. — **18**, No. 11. — P. 1845–1867.

[13] *Kobayashi N., Mieda T., Shiba H., Shinozaki Y.* A study of the liquid slosh response in horizontal cylindrical tanks // Transactions of the ASME. J. Pressure Vessel Technology. — 1989. — **111**. — P. 32–38.

[14] *Kolae A., Rakheja S., Richard M.J.* Range of applicability of the linear fluid slosh theory for predicting transient lateral slosh and roll stability of tank vehicles // J. of Sound and Vibration. — 2014. — **333**, No. 1. — P. 263–282.

[15] *Lukovsky I.A.* Nonlinear sloshing in tanks of complex geometrical shape. — Kiev: Nauk. Dumka, 1975 (in Russian). — 136 p.

[16] *Moderassi-Tehrani K., Rakheja S., Sedaghati R.* Analysis of the overturning moment caused by transient liquid slosh inside a partly filled moving tank // Proc. IMechE, Part D: J. of Automobile Engineering. — 2006. — **220**. — P. 289–301.

[17] *Moiseev N.N.* On the theory of nonlinear vibrations of a liquid of finite volume // J. of Applied Math. and Mechanics. — 1958. — **22**, No. 5. — P. 860–872.

[18] *Navarrete J.A.R., Cano O.R., Romero J.M.F., Hidebrand R., Madrid M.M.* Caracterizaciòn experimental del oleaje en tanquues. — Tech. Rep., Publication Technica No. 219. Instituto Mexicano del Transpote (IMT), 2003, Secretaria de Comunicaciones Y Transportes (SCT). — 120 p.

[19] *Ockendon J.R., Ockendon H., Waterhouse D.D.* Multi-mode resonance in fluids // J. of Fluid Mechanics. — 1996. — **315**. — P. 317–344.

[20] *Sames P.C., Marcouly D., Schellin T.E.* Sloshing in rectangular and cylindrical tanks // J. of Ship Research. — 2002. — **46**, No. 3. — P. 186–200.

[21] *Strandberg L.* Lateral sloshing of road tankers. Volume 1: Main report. — Tech. Rep., Nr 138A-1978. National Road and Traffic Research Institute, S-58101, Linköping, Sweden. — 250 p.